


Characterization of ytterbium resonance lines at 649 nm with modulation-transfer spectroscopy

Min Zhou, Sheng Zhang , Limeng Luo, and Xinye Xu *

State Key Laboratory of Precision Spectroscopy, East China Normal University, Shanghai 200062, China

 (Received 16 November 2019; revised manuscript received 19 April 2020; accepted 13 May 2020; published 3 June 2020)

We report modulation-transfer spectroscopy (MTS) on the $6s6p\ ^3P_0 \leftrightarrow 6s7s\ ^3S_1$ transition in neutral ytterbium (Yb) isotopes in a hollow cathode lamp. The MTS dispersive signals show an effective linewidth of 70 MHz, contributed primarily by the pressure broadening. MTS has demonstrated the capability of completely resolving all isotopic lines, except the one in low-abundance ^{168}Yb . Frequency measurements of the isotope-stabilized laser are performed using an optical comb, and systematic shifts therein are corrected. We have examined the relative isotope shifts, and the hyperfine constants for the $6s7s\ ^3S_1$ state are given as $A(^{171}\text{Yb}) = 6837.83(19)$ MHz, $A(^{173}\text{Yb}) = -1891.46(7)$ MHz and $B(^{173}\text{Yb}) = -0.62(16)$ MHz. Our results are in reasonable agreement with previously reported values and essentially resolve the existing discrepancies.

DOI: [10.1103/PhysRevA.101.062506](https://doi.org/10.1103/PhysRevA.101.062506)

I. INTRODUCTION

In recent years, neutral ytterbium (Yb) has attracted considerable experimental attention in the study of atomic parity nonconservation [1,2], optical atomic clocks [3–8], and quantum degenerate gases [9–12]. The $6s6p\ ^3P_0 \leftrightarrow 6s7s\ ^3S_1$ transition can be availably used as a repump transition among these applications. It would be of great interest to determine the accurate location of isotopic resonance lines, for example, for optimizing the normalized shelving detection in ^{171}Yb -based optical clocks. Furthermore, precise measurement of isotope shifts and hyperfine constants can provide important tests for atomic structure theory. There are, however, very few reports of frequency measurement on this transition. The only one was carried out by roughly aligning the laser to the absorption peaks [13]. Nevertheless, results therein lack the adequate discussion of systematic errors.

The $6s6p\ ^3P_0 \leftrightarrow 6s7s\ ^3S_1$ transition in Yb atoms is located at around 649 nm with a natural linewidth of $\gamma_n = 1.5$ MHz [14]. The absorption lines and the hyperfine structure have been investigated either by saturated absorption spectroscopy (SAS) or optogalvanic spectroscopy in a hollow cathode lamp (HCL) [13,15,16]. In these experiments, isotope shifts were determined by peak fitting of the scanned spectra, where the frequency scale was calibrated by a Fabry-Pérot (FP) interferometer with known free space range. Some disagreements of hyperfine constants exist between different measurements [15,17,18], which may be caused by the nonlinear laser scanning or the imperfect multipeak fitting.

In this article we characterize Yb spectral lines through laser frequency stabilization and precise frequency measurement. Active laser stabilization is implemented with modulation-transfer spectroscopy (MTS) [19,20] in the HCL. MTS is one of the highly sensitive Doppler-free spectroscopic techniques commonly used in absorption detection of He [21],

Li [22], K [23,24], Ca [25], Rb [26–28], Te₂ [29], I₂ [30,31], Cs [32,33], Ba⁺ [34], Ho [35], Er [36,37], Yb [38–40], etc. With the MTS technique, the frequency shift induced by the Doppler background signal can be sufficiently suppressed. It is worth noting that the above lines are often cycling transitions involving the ground state. To our knowledge, we here present the first demonstration of MTS on the Yb 649-nm line, which starts from the metastable state. Fully resolved dispersive signals with remarkable signal-to-noise ratio (SNR) can be readily generated for eight lines in all isotopes but ^{168}Yb . Further, the laser frequencies are measured against the hydrogen maser using an optical frequency comb, and systematic errors are also addressed. Therefore, the advance compared to all previous work is the ability to make direct precision frequency measurements, thus determining the isotope shifts as well as hyperfine constants with an enhanced reliability.

This article is organized as follows. Section II describes the experimental setup. In Sec. III we obtain the spectra of Yb resonance lines in the HCL. In particular, the MTS dispersive signals are prepared for laser frequency stabilization and the absolute measurement, followed by the determination of isotope shifts and hyperfine constants. Section IV summarizes our work and presents an outlook.

II. EXPERIMENTAL SETUP

Figure 1 shows a schematic of the experimental setup used in MTS. Ytterbium's low vapor pressure does not permit it to be used in a vapor cell at room temperature. Usually the ytterbium atomic gas is obtained from a heated oven or a vapor cell with temperature of several hundred Kelvin [41,42]. An HCL, which is well suited for performing spectroscopy in refractory elements such as Yb, can replace these complex apparatuses. The cathodic sputtering could populate Yb atoms on many metastable states by generating the discharge plasma, thus allowing possible observation of the 649-nm absorption.

*Corresponding author: xyxu@phy.ecnu.edu.cn

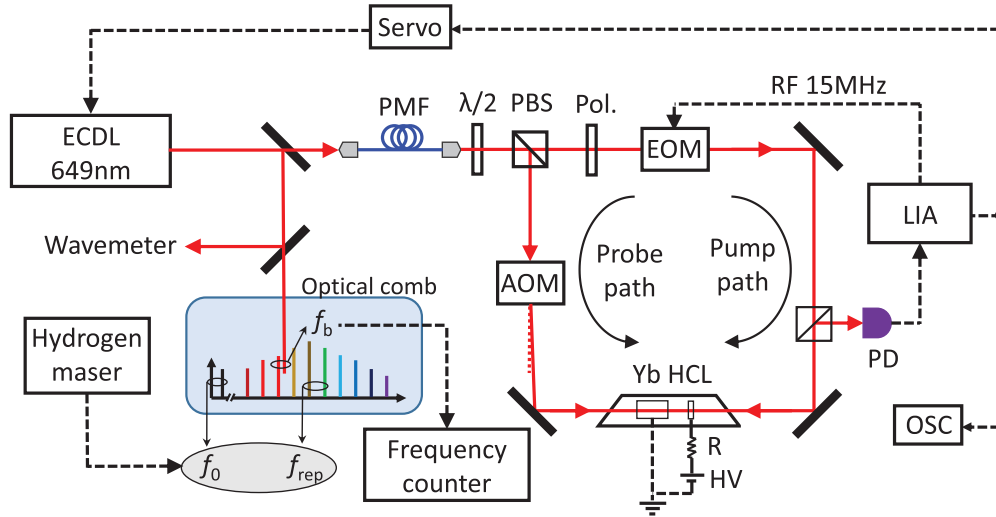


FIG. 1. Simplified schematic of the experimental setup for the modulation-transfer spectroscopy and the frequency measurement. Variant arrangements for saturated absorption spectroscopy and frequency modulation spectroscopy are described in the text. ECDL, external cavity diode laser; PMF, polarization maintaining fiber; $\lambda/2$, half-wave plate; PBS, polarization beam splitter; Pol., linear polarizer; EOM, electro-optic modulator; RF, radio frequency; LIA, lock-in amplifier; AOM, acousto-optic modulator; f_0 , carrier-envelope offset frequency of the comb; f_{rep} , repetition rate of the comb; f_b , heterodyne beat note between the comb and the 649-nm laser; HCL, hollow cathode lamp; PD, photodetector; R, ballast resistor; HV, high-voltage power supply; OSC, digital oscilloscope.

Nevertheless, it is still a challenge to obtain a fairly large optical depth (OD) of the medium since the fraction of atoms on the 3P_0 state could be very small. Here, the see-through HCL (Hamamatsu L2783-70Ne-Yb) is filled with the Ne buffer gas at a pressure of 5–10 Torr. The discharge is sustained by a dc high-voltage power supply with a 10-mA maximum current suggested by the manufacturer. A ballast resistor ($R = 47 \text{ k}\Omega$) is required to keep the discharge for stable operation.

An external cavity diode laser emitting at 649 nm is used as the light source. Its spectral bandwidth is comparable to the natural linewidth of the atomic transition. The laser is mainly divided into three beams. Tens of microwatts of laser power are connected to a wavemeter (HighFinesse WS7-60) for monitoring the laser mode hopping and coarsely recording the frequency. The second beam with about 4 mW power is sent to an optical comb for frequency measurement. The major power is delivered to the spectrometer (about 7 mW after delivery) through a polarization-maintaining fiber. The incident polarization is accurately aligned parallel with the slow axis of the fiber through a polarization analyzer. The pump and probe beams are generated by the polarization beam splitter and are collinearly counterpropagated in the HCL. Their relative power ratio can be controlled by the front $\lambda/2$ waveplate.

In the MTS experiment, the pump laser field is phase modulated through an electro-optic modulator (EOM) (Qubig EO-Tx16M3-NIR) resonant at 15 MHz, and the probe beam is frequency downshifted by 78 MHz with an acousto-optic modulator (AOM). The insertion of AOM prevents the possible mutual interference in the HCL [43]. To obtain a pure phase modulation, the beam polarization is aligned parallel to the optical axis of the EOM with a linear polarizer and the EOM is intentionally tilted with a slight angle [44]. Both sizes of the incident beams are adjusted to a diameter of about 3 mm, just fitting with the axial region of the discharge plasma. The electric signal from the fast photodetector, by

collecting the probe beam intensity of about 0.7 mW, is sent to a high-frequency digital lock-in amplifier (LIA) (Liquid Instruments Moku:Lab) for frequency demodulation. The cutoff frequency of the integrated low-pass filter is 50 Hz with a roll-off slope of 24 dB/octave. This LIA also provides the driving rf source for the EOM, where the modulation index is moderately set around 1.1 rad [45].

The obtained error signal is captured by a digital oscilloscope and is also sent to the servo system for laser feedback control. The optical frequency comb (MenloSystems FC1500-250-ULN) is based on a femtosecond Er-doped fiber laser. The primary source of light at 1560 nm passes a high-power amplifier and is converted to 780 nm using the integrated frequency-doubling module. Then the radiation is spectrally broadened by supercontinuum generation in a photonic crystal fiber. The carrier-envelope offset frequency (f_0) is derived from the common f -to- $2f$ interferometer [46]. f_0 and the repetition rate of the comb (f_{rep}) are both phase locked to the direct digital synthesizers (DDSs) at 35 and 250 MHz, respectively. The beat note (f_b) between the 649-nm laser and the comb is amplified and filtered before sending to the frequency counter (Stanford Research SR620). All rf signals are referenced to the common 10-MHz source from the hydrogen maser. The maser reference is calibrated with an absolute accuracy of about 1 part in 10^{12} via the GPS link with a time transfer system. It provides a short-term instability (Allan deviation) less than 2×10^{-13} at 1-s averaging time and attains the floor of about 3×10^{-15} over 500 s.

III. RESULTS AND DISCUSSION

A. Saturated absorption spectrum

Prior to performing the FMS and MTS experiments, the isotopic distribution is verified with conventional SAS.

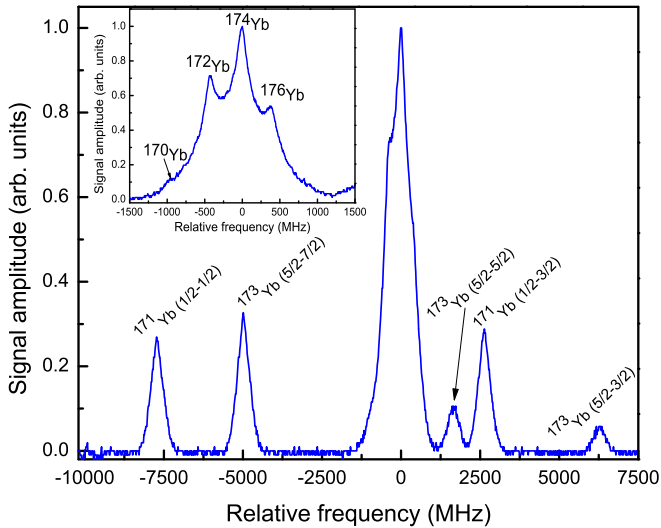


FIG. 2. Saturated absorption spectrum of the ytterbium isotopes observed in a hollow cathode lamp with about a 20-GHz scanning of the 649-nm laser. The frequencies are all relative to the ^{174}Yb isotope resonance. The inset shows the spectrum of four even isotopes with better resolution.

Compared with the MTS setup in Fig. 1, the AOM is swapped into the pump path and the EOM is removed. External amplitude modulation (AM) is applied on the AOM with a 100% modulation depth at frequency of 30 kHz. The absorption signal amplitude increases with the discharge current of the lamp, which is the direct consequence of increased OD of the ytterbium atoms. The current is set at 9 mA for compromise of a guaranteed discharge lifetime. Figure 2 shows a typical spectrum with a laser scan of about 20 GHz, which has also identified the isotope and the hyperfine structure according to previous work [13,15,16]. The frequency scale is calibrated by the two farthest peaks with their frequencies monitored by the wavemeter. There are no visible crossover isotopic resonances, thus simplifying the identification.

Spectral profiles in the odd isotopes are well resolved due to the large splitting of the hyperfine energy levels. Since there is only one ground state, hyperfine pumping [47] is absent for the 649-nm transition. Each peak has an inhomogeneous width of about 700 MHz by fitting to the sub-Doppler collision shape [48,49], corresponding to a Doppler width of Yb vapor at 900 K. The fitted homogeneous linewidth of about 120 MHz, which is substantially larger than the natural linewidth, arises from various broadening mechanisms such as the beam misalignment, the pressure, and the power effects [15]. The closely spaced lines with about 400 MHz separation in even isotopes cannot be completely resolved. With the fifth-harmonic detection by another LIA (Stanford Research SR830), the spectrum shows a better resolution, as shown in the inset of Fig. 2. Specifically, the feature of ^{170}Yb appears at around -934 MHz, in close agreement with the previous measurement [15]. The weak transition in ^{168}Yb is unsurprisingly obscured in the Doppler-free spectrum, since it has the lowest abundance of 0.13%.

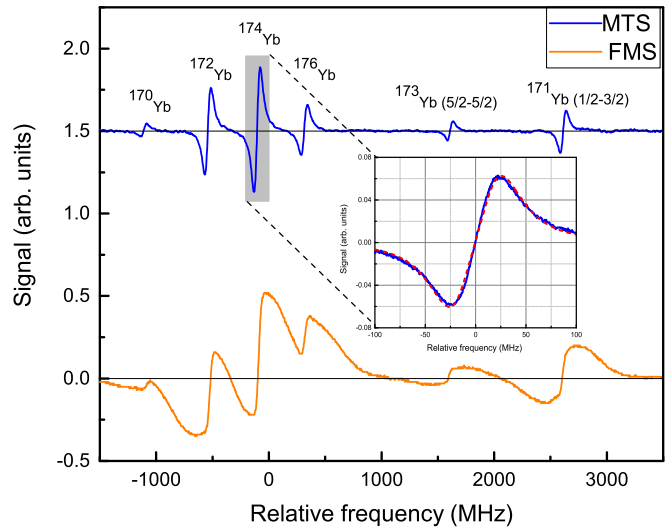


FIG. 3. Selected dispersive signals of the ytterbium isotopes in frequency modulation spectroscopy (FMS) and modulation-transfer spectroscopy (MTS). The MTS signal is intentionally offset from the zero baseline for visual clarity. The inset shows the ^{174}Yb signal without offset at higher resolution (blue solid line) and the theoretical fitting (red dashed line), where the observable width and the effective linewidth are 50 and 70(1) MHz, respectively.

B. Dispersive signals with MTS and FMS

To generate an antisymmetric dispersive signal with a steep zero-crossing in the SAS for laser frequency locking, the optical field is preferred to be phase or frequency modulated. In the MTS experiment, the pump laser field is phase modulated, whereas the counterpropagating probe laser is unmodulated. Modulation is transferred from the pump beam to the probe beam, and the MTS signals are well explained by the nonlinear four-wave mixing [20].

Apart from MTS, there is another frequently used technique termed frequency modulation spectroscopy (FMS) [50,51]. The arrangement in our FMS experiment has a superficial similarity to that in MTS (see Fig. 1), but they differ fundamentally in principle. As for FMS, the EOM is swapped with the AOM into the probe path for phase modulation. To suppress the baseline offset, amplitude modulation is imparted to the pump beam via the AOM with the same modulation parameters as used in SAS. The final signals are recovered with two LIAs, first by the frequency demodulation and subsequently by the amplitude demodulation.

Both the FMS and MTS experiments could yield dispersive signals, as shown in Fig. 3. Spectral profiles in the FMS have a comparable width to the MTS signals. However, the FMS still has a visible residual background, which results in different offsets of the locking point from the baseline in even isotopes. This phenomenon also occurs in other FMS experiments such as in Ref. [28], although it looks much worse in our case. The MTS signals show a spectacular improvement in resolution and also feature a flat baseline. Since all hyperfine transitions are closed, the odd-isotope signals are relatively strong as expected. In addition, the ^{170}Yb signal is completely distinguished from other isotopic components, and the peak position just coincides with that in the inset of Fig. 2.

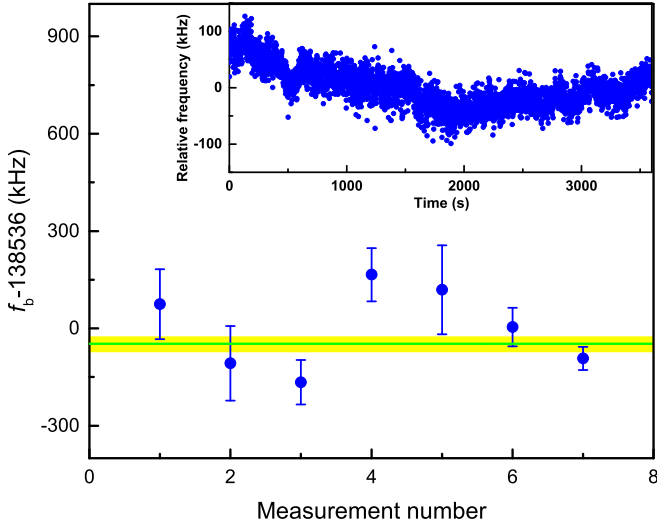


FIG. 4. The beat-note frequency of the laser stabilized on the $^{174}\text{Yb } 6s6p \ ^3P_0 \leftrightarrow 6s7s \ ^3S_1$ resonance and the comb. Each frequency data point is calculated from a one-hour recording. The inset shows the last frequency record. The green solid line is a linear fit with zero slope to seven data points. The yellow shaded band indicates the statistical uncertainty. All measurements are carried out with HCL current of 9 mA, pump power of 2.64 mW, and probe power of 1 mW (both measured just before the HCL).

MTS signals have an observable width of 50 MHz, as shown in the inset of Fig. 3. As we do not observe a clear correlation of the width with the lamp current at 6–9 mA or with the laser power (pump: 1–2.4 mW, probe: 0.36–0.9 mW), the broadening primarily comes from the pressure contribution. A deeper discussion about the pressure broadening is promoted in the next section. We will see pressure and power broadenings contribute factors of 45 and at most 8 in the linewidth, respectively. For all Yb isotopes but ^{168}Yb , MTS has the capability to provide clear dispersive signals in the HCL. As the four-wave mixing process only occurs under the sub-Doppler resonance condition, MTS signals have stable zero-crossings over time and are more suited as the frequency discriminant for laser frequency stabilization.

C. Frequency measurement and systematic errors

Closed-loop laser locking is implemented by regulating the laser diode electric current with the MTS dispersive signal. The diode laser can be reliably stabilized on the atomic resonances, even with relatively low SNR signals of ^{170}Yb , $^{173}\text{Yb}(5/2 - 5/2)$ and $^{173}\text{Yb}(5/2 - 3/2)$. The frequency counter records the individual beat note, and the optical frequency is calculated from

$$\nu = n f_{\text{rep}} \pm 2f_0 \pm f_b - 39 \text{ MHz}, \quad (1)$$

where n is the integer of the comb mode number. The factor 2 accounts for the doubling effect from the comb primary source. The ambiguous signs \pm can be removed by observing their change directions through slightly altering the DDS frequencies. The negative offset of 39 MHz is the necessary correction with one half the AOM frequency [43].

TABLE I. Systematic frequency shifts of the $6s6p \ ^3P_0 \leftrightarrow 6s7s \ ^3S_1$ transition in ^{174}Yb . RAM: residual amplitude modulation.

Effect	Shift (MHz)	Uncertainty (MHz)
Pressure	-14.0	3.2
Laser power	0.13	0.04
Lamp current	3.59	0.09
RAM	-0.12	0.08
Locking offset	0	0.08
Total	-10.4	3.2

Figure 4 shows seven frequency measurements of the beat note spanning one week. The average frequency is 138.489 MHz, with a statistical uncertainty of 25 kHz. Each data point contains a one-hour frequency recording on the counter with 1-s gate time. The vertical error bar ranges from 36 to 137 kHz, which corresponds to a relative statistical uncertainty of $3 \times 10^{-4} \sim 1 \times 10^{-3}$. We attribute it to the environmental temperature fluctuation and air disturbance. The beat note gets more stable when the experimental setup is placed into the acrylic enclosure. A typical improved recording is shown in the inset of Fig. 4.

The systematic shifts and their uncertainty budgets in ^{174}Yb are listed in Table I. Since the buffer gas pressure in the HCL is not exactly specified, we estimate it from the effective linewidth of $\gamma_e = 70(1)$ MHz in MTS signals (see the inset of Fig. 3). γ_e is a combined linewidth of power and pressure broadening (γ_p) and can be described by [52]

$$\gamma_e = \gamma_n \sqrt{\frac{I}{I_{\text{sat}}} + \left(1 + \frac{\gamma_p}{\gamma_n}\right)^2}, \quad (2)$$

where I is the laser intensity, and I_{sat} is the saturation intensity of 0.74 mW/cm^2 . I/I_{sat} is less than 60 in our experiments, and then we find γ_p is 67.5 MHz from Eq. (2). Using the broadening rate in Ref. [53], we expect a pressure of 5.4(7) Torr, meeting the specification of 5–10 Torr. The pressure shift coefficient was given as $-2.6(5)$ MHz/Torr at 22°C for the Ne buffer gas [53]. Therefore, the pressure shift is $-14.0(32)$ MHz. We measure the dependences of the frequency on the laser power and the lamp current. As shown in Fig. 5(a), these quoted laser powers have taken into account a loss of 10% at each glass surface of the HCL. It seems the frequency has little or almost no correlation with the laser power. The frequency shift due to the HCL current has a linear trend with a slope of $0.40(1)$ MHz/mA, as shown in Fig. 5(b). Extrapolation of the data to zero current gives a shift of $3.59(9)$ MHz.

MTS signals may suffer from minor distortion by the residual amplitude modulation (RAM) [54–56]. By fitting the dispersive signal, the ratio between the AM and FM sideband amplitudes is less than 0.1%, as shown in the inset of Fig. 3. The frequency shift is estimated to be $-0.12(8)$ MHz, where the beam misalignment has been already included as a balanced effect [55,56]. The zero-crossing point in each locking phase is carefully chosen with an offset uncertainty of 0.2 mV in the LIA controller, which could make a frequency inaccuracy of 83 kHz for an error signal of 120 mV (peak-to-peak amplitude). The metal cathode in the discharge region of the HCL has a magnetic attenuation factor of 2–3 [57,58],

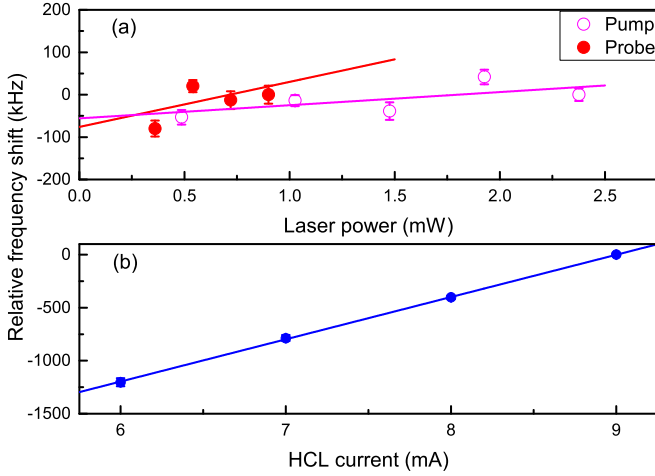


FIG. 5. Relative frequency shift of the beat note with (a) laser power and (b) HCL current. The solid lines are the linear fittings.

and no attempt is made to null the residual magnetic field in the lamp. We are aware it has an insignificant effect on our measurements. The errors from the comb system and the maser reference are also negligible. According to Eq. (1) and taking all systematic uncertainties into account, the absolute frequency of ^{174}Yb is determined to be $\nu = 461, 868, 929.9 \pm 3.2$ MHz.

In this manner, absolute frequencies of other isotopes are figured out and they are summarized in Table II. The only previous measurement of these frequencies was reported in Ref. [13], where the absorption-peak frequencies were tracked by a spectrum analyzer without laser locking. Our results disagree with these values by about 54–86 MHz, which are one or two times their uncertainties. None of the error sources we have evaluated can account for these discrepancies. This is probably attributable to their imprecise determination of resonance peaks, which are still broad with SAS.

D. Isotope shifts and hyperfine constants

Given that the same HCL are operated under identical conditions, the dominating pressure shift would be the same for different isotopes. Moreover, we have observed in experiments that the frequency dependencies on the laser power

TABLE II. Absolute frequencies of the $6s6p\ ^3P_0 \leftrightarrow 6s7s\ ^3S_1$ transition lines. Systematic shifts are corrected to give the center frequency. The given transitions have a common absolute uncertainty of 3.2 MHz due to combined statistical and systematic uncertainties.

Line	Center frequency (MHz)
$^{171}\text{Yb}(1/2 - 1/2)$	461 861 338.1
$^{173}\text{Yb}(5/2 - 7/2)$	461 863 970.9
^{170}Yb	461 867 981.9
^{172}Yb	461 868 512.3
^{174}Yb	461 868 929.9
^{176}Yb	461 869 328.3
$^{173}\text{Yb}(5/2 - 5/2)$	461 870 590.3
$^{171}\text{Yb}(1/2 - 3/2)$	461 871 594.9
$^{173}\text{Yb}(5/2 - 3/2)$	461 875 319.7

TABLE III. Isotope shifts and hyperfine splittings for the $6s6p\ ^3P_0 \leftrightarrow 6s7s\ ^3S_1$ transition lines. All data are given in units of megahertz, and their corresponding one-standard-deviation uncertainties are given in parentheses.

Line	Ref. [15]	This work
$^{171}\text{Yb}(1/2 - 1/2)$	-7568(33)	-7591.77(21)
$^{173}\text{Yb}(5/2 - 7/2)$	-4926(50)	-4959.02(20)
^{170}Yb	-937(29)	-947.85(24)
^{172}Yb	-413(20)	-417.56(20)
^{174}Yb	0	0
^{176}Yb	+392(26)	+398.37(20)
$^{173}\text{Yb}(5/2 - 5/2)$	+1651(59)	+1660.45(21)
$^{171}\text{Yb}(1/2 - 3/2)$	+2647(32)	+2664.97(20)
$^{173}\text{Yb}(5/2 - 3/2)$	+6349(55)	+6389.80(22)

and the HCL current behave almost the same for different isotopes, respectively. Based on Table II, relative isotope shifts are calculated in Table III. Previously reported results of another group [15] are included as well for comparison. Our measurements agree well with the spectral fitting results but improve the accuracy by factors of 60–190.

The hyperfine frequency shift with respect to the unperturbed level is associated with the magnetic dipole and electric quadrupole interactions [59]:

$$\nu_{hfs} = \frac{1}{2}AK + B \frac{\frac{3}{2}K(K+1) - 2I(I+1)J(J+1)}{2I(2I-1)2J(2J-1)}, \quad (3)$$

where $K = F(F+1) - I(I+1) - J(J+1)$, with A the magnetic dipole constant, B the electric quadrupole constant, F the quantum number of the total angular momentum $\mathbf{F} = \mathbf{I} + \mathbf{J}$, I the quantum number of the nuclear angular momentum, and J the quantum number of the total electronic angular momentum. There are two isotopes in Yb with nonzero nuclear spin: ^{171}Yb ($I = 1/2$) and ^{173}Yb ($I = 5/2$). Since the upper $6s7s\ ^3S_1$ state has $J=1$, one can get $F = \{1/2, 3/2\}$ for ^{171}Yb and $F = \{3/2, 5/2, 7/2\}$ for ^{173}Yb , respectively.

The hyperfine constants can be deduced from the hyperfine frequency shifts in Table II after some algebraic calculations according to Eq. (3). Our results are compared with previous measurements in Table IV and Fig. 6. For $A(^{171}\text{Yb})$, there is an apparent discrepancy between Ref. [15] and others. Meanwhile, the two results [17,18] are almost completely scattered outside their uncertainties. Our result is in good agreement with Ref. [17] but disagrees with the most precise

TABLE IV. Hyperfine constants of ^{171}Yb and ^{173}Yb for the $6s7s\ ^3S_1$ state. All data are given in units of megahertz, and their corresponding one-standard-deviation uncertainties are given in parentheses.

$A(^{171}\text{Yb})$	$A(^{173}\text{Yb})$	$B(^{173}\text{Yb})$	Reference
6860	-1900	< 10	[60]
6857.2	-1892.2	0	[61]
6837(9)	-1894(8)	/	[17]
6810(10)	-1879(10)	< -3(18)	[15]
6847.7(17)	-1892.78(42)	-0.2(10)	[18]
6837.83(19)	-1891.46(7)	-0.62(16)	This work

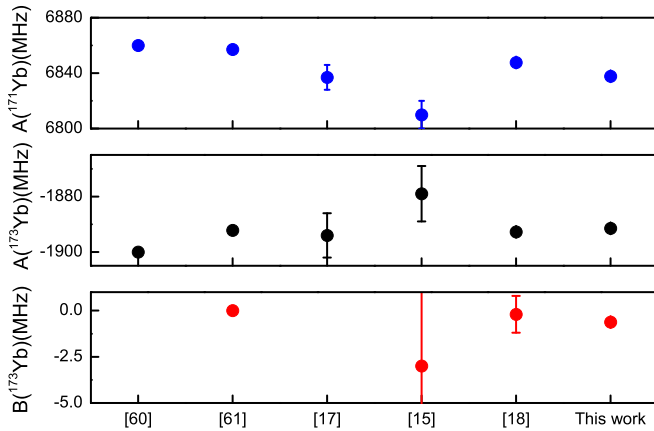


FIG. 6. Summary of the hyperfine constants for the 649-nm line in Yb. We make comparisons with previous measurements.

measurement reported previously by six times the combined uncertainties [18]. As noted previously, we suspect that this discrepancy might result from the nonlinear laser scanning or imperfect spectral fittings in Ref. [18]. $A(^{173}\text{Yb})$ in this work agrees well with the previous value [17] but differs from that in Refs. [15, 18]. Our new value for $B(^{173}\text{Yb})$ is in reasonable agreement with all previously reported results but has a much smaller uncertainty.

IV. SUMMARY

In summary, we perform MTS in an HCL to carry out absolute frequency measurements of the 649-nm transition

lines in Yb isotopes using the optical comb. We have also examined the isotope shifts and hyperfine constants. The absolute frequencies and the isotope shifts are at least one order of magnitude more accurate than previous measurements, which are useful to atomic physics experiments. Our hyperfine constants also resolve some discrepancies between previously reported values.

We have investigated the systematic errors from the pump power, the probe power, and the HCL current. The RAM shifts induced by the unwanted AM and the beam misalignment are corrected together by fitting the MTS signal shape. The pressure shift, which comes from collisions of Yb atoms with the Ne buffer gas in the HCL, dominates all other sources of error. Further developments can be expected in the direction of frequency calibration by other sources, such as the Yb atomic beam method, by comparing absorption profiles in the vapor cell with fluorescence data [62].

ACKNOWLEDGMENTS

This work was supported by the National Key Basic Research and Development Program of China (Grants No. 2017YFF0212003, No. 2016YFA0302103, and No. 2016YFB0501601), Shanghai Municipal Science and Technology Major Project (Grant No. 2019SHZDZX01), the National High Technology Research and Development Program of China (Grant No. 2014AA123401), the National Natural Science Foundation of China (Grant No. 11134003), and Shanghai Excellent Academic Leaders Program of China (Grant No. 12XD1402400).

-
- [1] K. Tsigtukin, D. Dounas-Frazer, A. Family, J. E. Stalnaker, V. V. Yashchuk, and D. Budker, Observation of a Large Atomic Parity Violation Effect in Ytterbium, *Phys. Rev. Lett.* **103**, 071601 (2009).
- [2] D. Antypas, A. Fabricant, J. E. Stalnaker, K. Tsigtukin, V. V. Flambaum, and D. Budker, Isotopic variation of parity violation in atomic ytterbium, *Nat. Phys.* **15**, 120 (2019).
- [3] C. Y. Park, D.-H. Yu, W.-K. Lee, S. E. Park, E. B. Kim, S. K. Lee, J. W. Cho, T. H. Yoon, J. Mun, S. J. Park, T. Y. Kwon, and S.-B. Lee, Absolute frequency measurement of $^1S_0(F=1/2)$ – $^3P_0(F=1/2)$ transition of ^{171}Yb atoms in a one-dimensional optical lattice at KRISS, *Metrologia* **50**, 119 (2013).
- [4] N. Nemitz, T. Ohkubo, M. Takamoto, I. Ushijima, M. Das, N. Ohmae, and H. Katori, Frequency ratio of Yb and Sr clocks with 5×10^{-17} uncertainty at 150 seconds averaging time, *Nat. Photonics* **10**, 258 (2016).
- [5] M. Pizzocaro, P. Thoumany, B. Rauf, F. Bregolin, G. Milani, C. Clivati, G. A. Costanzo, F. Levi, and D. Calonico, Absolute frequency measurement of the 1S_0 – 3P_0 transition of ^{171}Yb , *Metrologia* **54**, 102 (2017).
- [6] Q. Gao, M. Zhou, C. Han, S. Li, S. Zhang, Y. Yao, B. Li, H. Qiao, D. Ai, G. Lou, M. Zhang, Y. Jiang, Z. Bi, L. Ma, and X. Xu, Systematic evaluation of a ^{171}Yb optical clock by synchronous comparison between two lattice systems, *Sci. Rep.* **8**, 8022 (2018).
- [7] T. Kobayashi, D. Akamatsu, Y. Hisai, T. Tanabe, H. Inaba, T. Suzuyama, F. Hong, K. Hosaka, and M. Yasuda, Uncertainty evaluation of an ^{171}Yb optical lattice clock at NMIJ, *IEEE Trans. Ultrason. Ferroelectr. Freq. Control* **65**, 2449 (2018).
- [8] W. F. McGrew, X. Zhang, H. Leopardi, R. J. Fasano, D. Nicolodi, K. Beloy, J. Yao, J. A. Sherman, S. A. Schäffer, J. Savory, R. C. Brown, S. Römisch, C. W. Oates, T. E. Parker, T. M. Fortier, and A. D. Ludlow, Towards the optical second: Verifying optical clocks at the SI limit, *Optica* **6**, 448 (2019).
- [9] T. Fukuhara, S. Sugawa, and Y. Takahashi, Bose-Einstein condensation of an ytterbium isotope, *Phys. Rev. A* **76**, 051604(R) (2007).
- [10] T. Fukuhara, Y. Takasu, M. Kumakura, and Y. Takahashi, Degenerate Fermi Gases of Ytterbium, *Phys. Rev. Lett.* **98**, 030401 (2007).
- [11] A. Khrarov, A. Hansen, W. Dowd, R. J. Roy, C. Makrides, A. Petrov, S. Kotochigova, and S. Gupta, Ultracold Heteronuclear Mixture of Ground and Excited State Atoms, *Phys. Rev. Lett.* **112**, 033201 (2014).
- [12] R. Yamamoto, J. Kobayashi, T. Kuno, K. Kato, and Y. Takahashi, An ytterbium quantum gas microscope with narrow-line laser cooling, *New J. Phys.* **18**, 023016 (2016).
- [13] A. Yamaguchi, Metastable state of ultracold and quantum degenerate ytterbium atoms: High-resolution spectroscopy and cold collisions, Ph.D. thesis, Kyoto University, 2008.

- [14] J. W. Cho, H.-G. Lee, S. Lee, J. Ahn, W.-K. Lee, D.-H. Yu, S. K. Lee, and C. Y. Park, Optical repumping of triplet- p states enhances magneto-optical trapping of ytterbium atoms, *Phys. Rev. A* **85**, 035401 (2012).
- [15] R. W. Berends and L. Maleki, Hyperfine structure and isotope shifts of transitions in neutral and singly ionized ytterbium, *J. Opt. Soc. Am. B* **9**, 332 (1992).
- [16] D. F. Kimball, Collisional perturbation of states in atomic ytterbium, Undergraduate thesis, University of California at Berkeley, 1998.
- [17] C. Schulz, E. Arnold, W. Borchers, W. Neu, R. Neugart, M. Neuroth, E. W. Otten, M. Scherf, K. Wendt, P. Lievens, Y. A. Kudryavtsev, V. S. Letokhov, V. I. Mishin, and V. V. Petrunin, Resonance ionization spectroscopy on a fast atomic ytterbium beam, *J. Phys. B: At., Mol. Opt. Phys.* **24**, 4831 (1991).
- [18] T. Wakui, W.-G. Jin, K. Hasegawa, H. Uematsu, T. Minowa, and H. Katsuragawa, High-resolution diode-laser spectroscopy of the rare-earth elements, *J. Phys. Soc. Jpn.* **72**, 2219 (2003).
- [19] G. Camy, C. Bordé, and M. Ducloy, Heterodyne saturation spectroscopy through frequency modulation of the saturating beam, *Opt. Commun.* **41**, 325 (1982).
- [20] J. H. Shirley, Modulation transfer processes in optical heterodyne saturation spectroscopy, *Opt. Lett.* **7**, 537 (1982).
- [21] W. Gong, X. Peng, W. Li, and H. Guo, Frequency stabilization of a 1083 nm fiber laser to 4He transition lines with optical heterodyne saturation spectroscopies, *Rev. Sci. Instrum.* **85**, 073103 (2014).
- [22] D. Sun, C. Zhou, L. Zhou, J. Wang, and M. Zhan, Modulation transfer spectroscopy in a lithium atomic vapor cell, *Opt. Express* **24**, 10649 (2016).
- [23] L. Mudarikwa, K. Pahwa, and J. Goldwin, Sub-Doppler modulation spectroscopy of potassium for laser stabilization, *J. Phys. B: At., Mol. Opt. Phys.* **45**, 065002 (2012).
- [24] A. Arias, S. Helmrich, C. Schweiger, L. Ardizzone, G. Lochead, and S. Whitlock, Versatile, high-power 460 nm laser system for Rydberg excitation of ultracold potassium, *Opt. Express* **25**, 14829 (2017).
- [25] J. F. Eble and F. Schmidt-Kaler, Optimization of frequency modulation transfer spectroscopy on the calcium 4^1S_0 to 4^1P_1 transition, *Appl. Phys. B* **88**, 563 (2007).
- [26] N. Ito, Doppler-free modulation transfer spectroscopy of rubidium $5^2S_{1/2} - 6^2P_{1/2}$ transitions using a frequency-doubled diode laser blue-light source, *Rev. Sci. Instrum.* **71**, 2655 (2000).
- [27] J. Zhang, D. Wei, C. Xie, and K. Peng, Characteristics of absorption and dispersion for rubidium D2 lines with the modulation transfer spectrum, *Opt. Express* **11**, 1338 (2003).
- [28] D. J. McCarron, S. A. King, and S. L. Cornish, Modulation transfer spectroscopy in atomic rubidium, *Meas. Sci. Technol.* **19**, 105601 (2008).
- [29] T. Dutta, D. D. Munshi, and M. Mukherjee, Absolute Te_2 reference for barium ion at 455.4 nm, *J. Opt. Soc. Am. B* **33**, 1177 (2016).
- [30] M. L. Eickhoff and J. L. Hall, Optical frequency standard at 532 nm, *IEEE Trans. Instrum. Meas.* **44**, 155 (1995).
- [31] F.-L. Hong and J. Ishikawa, Hyperfine structures of the R(122)35-0 and P(84)33-0 transitions of $^{127}\text{I}_2$ near 532 nm, *Opt. Commun.* **183**, 101 (2000).
- [32] F. Bertinetto, P. Cordiale, G. Galzerano, and E. Bava, Frequency stabilization of DBR diode laser against Cs absorption lines at 852 nm using the modulation transfer method, *IEEE Trans. Instrum. Meas.* **50**, 490 (2001).
- [33] Z. Xu, X. Peng, L. Li, Y. Zhou, X. Qiu, D. Zhang, M. Zhou, and X. Xu, Modulation transfer spectroscopy for frequency stabilization of 852nm DBR diode lasers, *Laser Phys.* **30**, 025701 (2020).
- [34] C. Raab, J. Bolle, H. Oberst, J. Eschner, F. Schmidt-Kaler, and R. Blatt, Diode laser spectrometer at 493Å nm for single trapped Ba^+ ions, *Appl. Phys. B* **67**, 683 (1998).
- [35] J. Miao, J. Hostetter, G. Stratis, and M. Saffman, Magneto-optical trapping of holmium atoms, *Phys. Rev. A* **89**, 041401(R) (2014).
- [36] A. Frisch, K. Aikawa, M. Mark, A. Rietzler, J. Schindler, E. Zupanič, R. Grimm, and F. Ferlaino, Narrow-line magneto-optical trap for erbium, *Phys. Rev. A* **85**, 051401(R) (2012).
- [37] A. Frisch, K. Aikawa, M. Mark, F. Ferlaino, E. Berseneva, and S. Kotochigova, Hyperfine structure of laser-cooling transitions in fermionic erbium-167, *Phys. Rev. A* **88**, 032508 (2013).
- [38] W.-L. Wang and X.-Y. Xu, A novel method to measure the isotope shifts and hyperfine splittings of all ytterbium isotopes for a 399-nm transition, *Chin. Phys. B* **19**, 123202 (2010).
- [39] W.-L. Wang, J. Ye, H.-L. Jiang, Z.-Y. Bi, L.-S. Ma, and X.-Y. Xu, Frequency stabilization of a 399-nm laser by modulation transfer spectroscopy in an ytterbium hollow cathode lamp, *Chin. Phys. B* **20**, 013201 (2011).
- [40] T. Tanabe, D. Akamatsu, H. Inaba, S. Okubo, T. Kobayashi, M. Yasuda, K. Hosaka, and F.-L. Hong, A frequency-stabilized light source at 399 nm using an Yb hollow-cathode lamp, *Jpn. J. Appl. Phys.* **57**, 062501 (2018).
- [41] D. Antypas, A. Fabricant, L. Bougas, K. Tsigutkin, and D. Budker, Towards improved measurements of parity violation in atomic ytterbium, *Hyperfine Interact.* **238**, 21 (2017).
- [42] B. DeBoo, D. F. Kimball, C.-H. Li, and D. Budker, Multi-channel conical emission and parametric and nonparametric nonlinear optical processes in ytterbium vapor, *J. Opt. Soc. Am. B* **18**, 639 (2001).
- [43] J. J. Snyder, R. K. Raj, D. Bloch, and M. Ducloy, High-sensitivity nonlinear spectroscopy using a frequency-offset pump, *Opt. Lett.* **5**, 163 (1980).
- [44] E. A. Whittaker, M. Gehrtz, and G. C. Bjorklund, Residual amplitude modulation in laser electro-optic phase modulation, *J. Opt. Soc. Am. B* **2**, 1320 (1985).
- [45] E. Jaatinen, Theoretical determination of maximum signal levels obtainable with modulation transfer spectroscopy, *Opt. Commun.* **120**, 91 (1995).
- [46] D. J. Jones, S. A. Diddams, J. K. Ranka, A. Stentz, R. S. Windeler, J. L. Hall, and S. T. Cundiff, Carrier-envelope phase control of femtosecond mode-locked lasers and direct optical frequency synthesis, *Science* **288**, 635 (2000).
- [47] D. A. Smith and I. G. Hughes, The role of hyperfine pumping in multilevel systems exhibiting saturated absorption, *Am. J. Phys.* **72**, 631 (2004).
- [48] P. W. Smith and R. Hänsch, Cross-Relaxation Effects in the Saturation of the 6328-Å Neon-Laser Line, *Phys. Rev. Lett.* **26**, 740 (1971).
- [49] D. E. Thornton, G. T. Phillips, and G. P. Perram, Velocity changing collisions in the laser saturation spectra of $^{87}\text{Rb D}_2\text{F}'' = 2$, *Opt. Commun.* **284**, 2890 (2011).

- [50] G. C. Bjorklund, M. D. Levenson, W. Lenth, and C. Ortiz, Frequency modulation (FM) spectroscopy, *Appl. Phys. B* **32**, 145 (1983).
- [51] M. A. Norcia and J. K. Thompson, Simple laser stabilization to the strontium ^{88}Sr transition at 707 nm, *Rev. Sci. Instrum.* **87**, 023110 (2016).
- [52] U. Dammalapati, I. Norris, and E. Riis, Saturated absorption spectroscopy of calcium in a hollow-cathode lamp, *J. Phys. B: At., Mol. Opt. Phys.* **42**, 165001 (2009).
- [53] D. F. Kimball, D. Clyde, D. Budker, D. DeMille, S. J. Freedman, S. Rochester, J. E. Stalnaker, and M. Zolotarev, Collisional perturbation of states in atomic ytterbium by helium and neon, *Phys. Rev. A* **60**, 1103 (1999).
- [54] E. Jaatinen and J.-M. Chartier, Possible influence of residual amplitude modulation when using modulation transfer with iodine transitions at 543 nm, *Metrologia* **35**, 75 (1998).
- [55] E. Jaatinen, D. J. Hopper, and J. Back, Residual amplitude modulation mechanisms in modulation transfer spectroscopy that use electro-optic modulators, *Meas. Sci. Technol.* **20**, 025302 (2008).
- [56] E. Jaatinen and D. J. Hopper, Compensating for frequency shifts in modulation transfer spectroscopy caused by residual amplitude modulation, *Opt. Lasers Eng.* **46**, 69 (2008).
- [57] J. I. Kim, C. Y. Park, J. Y. Yeom, E. B. Kim, and T. H. Yoon, Frequency-stabilized high-power violet laser diode with an ytterbium hollow-cathode lamp, *Opt. Lett.* **28**, 245 (2003).
- [58] D. Pan, X. Xue, H. Shang, B. Luo, J. Chen, and H. Guo, Hollow cathode lamp based Faraday anomalous dispersion optical filter, *Sci. Rep.* **6**, 29882 (2016).
- [59] E. Arimondo, M. Inguscio, and P. Violino, Experimental determinations of the hyperfine structure in the alkali atoms, *Rev. Mod. Phys.* **49**, 31 (1977).
- [60] H. Schüler, J. Roig, and H. Korsching, Mechanische momente von $^{171,173}\text{Yb}$, quadrupolmoment von ^{173}Yb und häufigkeitsverhältnis von $^{173}\text{Yb} / ^{171}\text{Yb}$, *Z. Phys.* **111**, 165 (1938).
- [61] J. S. Ross and K. Murakawa, Nuclear moments of Yb^{173} , *J. Phys. Soc. Jpn.* **19**, 249 (1964).
- [62] M. Kleinert, M. E. Gold Dahl, and S. Bergeson, Measurement of the $\text{Yb I } ^1\text{S}_0 - ^1\text{P}_1$ transition frequency at 399 nm using an optical frequency comb, *Phys. Rev. A* **94**, 052511 (2016).